RESEARCH ON AN INTELLIGENT PREDICTION METHOD FOR THE STRESS FIELD IN PERFORATED CONCRETE SLABS BASED ON CONVOLUTIONAL NEURAL NETWORKS

Mou Nan[1]，Zheltkovich Andrei[2]

[1]аспирантура，Brest State Technical University，

Brest,Belarus,mounan1234@yeah.net，+375255268967

[2] PhD , Associate Professor,Brest State Technical University

Abstract: Finite-element (FE) analysis is the standard for stress evaluation in perforated concrete slabs, yet its run-time grows rapidly with geometric complexity. This study develops a convolutional neural-network (CNN) surrogate that predicts slab stress fields directly from geometry. Training targets are generated from a parametric FE model that enumerates hole layouts, including symmetric and asymmetric patterns, under shrinkage and service load combinations. To broaden geometric coverage, the dataset is expanded via generative augmentation (DCGAN) and procedural perturbations of hole geometry and spacing. On held-out geometries, the CNN reproduces FE stress with a Pearson correlation of 0.908 and an RMSE of 0.058 MPa for symmetric layouts, while delivering more than 50× faster inference than FE. Case studies on multi-hole slabs indicate that the surrogate remains accurate near re-entrant corners and narrow ligaments where stress gradients are steep, enabling rapid "what-if" exploration and efficient crack-resistance sizing. The proposed FE-supervised learning framework provides a direct and consistent comparison between the FE baseline and the neural surrogate, offering a practical path to real-time design support for large slabs with complex perforations.

Keywords: perforated concrete slabs; finite-element benchmark; convolutional neural networks; stress-field prediction; generative geometry augmentation.

INTRODUCTION

Large perforated concrete slabs used in industrial floors and equipment foundations exhibit pronounced stress concentrations under shrinkage and service actions. Empirical equivalent-stiffness reductions, though common in practice, can cause errors of 25–35% [1]. Finite-element (FE) analysis remains the reference for complex perforation layouts, but high-fidelity meshing, local refinement near re-entrant corners, and parameter sweeps over asymmetric patterns are time-consuming for routine design [2]. Recent data-driven surrogates offer an alternative: convolutional neural networks (CNNs) can learn mappings from geometry to stress fields when trained with reliable supervision [3–4]. Following this paradigm, we generate labeled stress fields from a parametric FE baseline spanning symmetric and asymmetric openings and use them to train a CNN surrogate. The resulting model reproduces FE response with high accuracy while enabling rapid "what-if" exploration and efficient crack-resistance sizing for large slabs with complex perforations.

MATERIALS AND METHODS

1. Finite-Element Baseline and Data Generation

1.1 Specimen Design and Monitoring Scheme

Geometry:A 4 × 4 × 0.25 m slab (C30–C50) is modeled with three hole configurations: (1) solid plate (control); (2) centrally-perforated plates with aperture

ratios 0.2/0.4; (3) eccentrically-perforated plates with eccentricities 0.5 m/1.0 m. For each configuration, multiple geometric realizations are generated to cover fabrication tolerances and layout variability. Hole surfaces are idealized as smooth in the FE model; typical physical hole-wall roughness (≈ Ra 25 μm) is noted for reference [3].

Boundary conditions and shrinkage: In-plane restraint conditions replicate floor-type edge restraint. Autogenous/drying shrinkage is represented by an equivalent eigen-strain (thermal analogy), applied in quasi-static steps. Material grade (C30–C50) is reflected by ranges of elastic modulus and tensile parameters.

Virtual instrumentation: Full-field strain and stress are exported from the FE solution and sampled with a regular evaluation grid over the slab surface, analogous to DIC-style field measurements [3], and circumferential line-probes within 1 m of each opening, analogous to FBG channel layouts used in structural monitoring [4]. These virtual probes provide consistent supervisory labels for learning and allow direct FE–CNN comparison on identical geometric inputs.

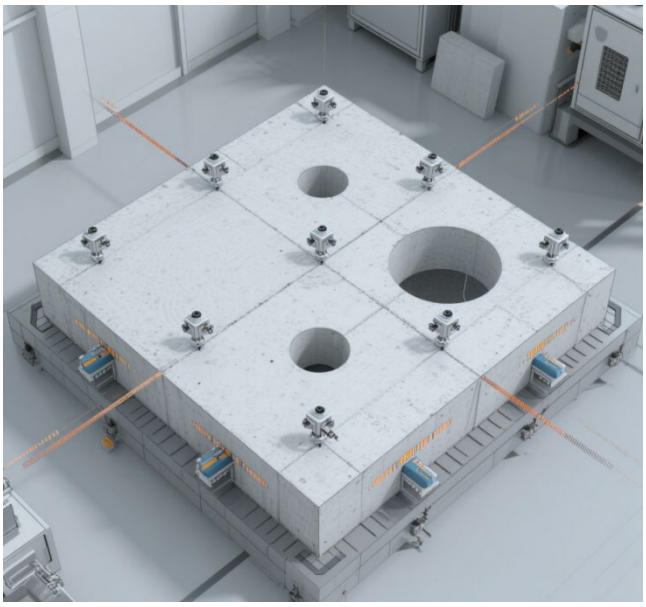

Figure 1. FE baseline geometry, loading/constraint idealization, and locations of virtual probes used for data export (conceptual schematic).

2. Salient features of the FE-supervised dataset

Field characteristics. The FE baseline shows that shrinkage-driven strain at the edge of a central opening is typically 25–30% higher than at the plate edge; the near-hole gradient increases sharply with aperture ratio, consistent with classical perforation effects. For an eccentricity of 1.0 m, peak principal stress shifts about 1.2 m from the geometric center, and the stress-concentration factor rises by 40% relative to the central-hole case [5].

Dataset composition. A parametric sweep over geometry (aperture ratio, eccentricity), material ranges (cement content, elastic modulus), and restraint conditions yields a multi-dimensional set of labeled stress fields sampled on a 16 × 16 grid, totaling 6,300 samples. These FE-supervised labels constitute the ground truth for training and validation of the CNN surrogate, ensuring a direct and consistent comparison to the FE baseline.

3. Construction and Optimization of the Convolutional Neural Network Model

3.1 Model Architecture Design

A U-Net encoder–decoder is adopted to map geometry/material descriptors to the target stress field on a 16×16 grid. Inputs consist of normalized geometric parameters (slab length, width, thickness, aperture, eccentricity) and material parameters (cement dosage, fly-ash content); these vectors are broadcast to spatial channels and concatenated with positional encodings so the network can resolve local gradients near openings. The decoder outputs the principal-stress field on the evaluation grid.

Key design choices are:

Dilated convolutions. Encoder blocks include dilated convolutions (rate = 2) to enlarge the receptive field and capture steep gradients around hole edges while keeping the parameter count modest.

Skip connections. U-Net skip paths fuse shallow geometric cues with deeper features to sharpen local predictions in narrow ligaments and re-entrant corners.

Physics-guided regularization. An equilibrium residual penalty enforces consistency with linear elasticity ($\nabla\cdot\sigma = 0$ in the absence of body forces) by adding a physics term to the loss, following the mechanics-constrained learning idea in [6]. The training objective is:

$$L=MSE(\sigma\hat{},\sigma FE)+\lambda Leq$$

where $\sigma^{FE}$are FE-supervised labels and $L_{eq}$is the divergence residual computed on the grid; $\lambda$is tuned on the validation set.

3.2 Data Augmentation and Training Strategy

Generative augmentation. To enrich asymmetric layouts, a DCGAN generates 1,000 virtual cases covering aperture 0.5–1.5 m and eccentricity 0–1.5 m. Generated samples are mixed with FE-baseline data at a 3:7 ratio during training to improve generalization to irregular geometries [7].

Optimization protocol. Training uses Adam with an initial learning rate of 1×10^{-4}, cosine decay, and early stopping based on validation RMSE. The dataset is split 70%/20%/10% for training/validation/testing.

Baselines for comparison. Performance is benchmarked against (i) the reference FE solution (Abaqus; eight-node quadrilateral elements; nominal mesh size 0.1 m) and (ii) the ACI-209 empirical approach for shrinkage-driven effects. Metrics include RMSE and Pearson correlation computed on held-out layouts, ensuring a direct and consistent FE–CNN comparison.

RESULTS

4.1 Model Performance Evaluation

For centrally perforated slabs with an aperture ratio of 0.4, the CNN surrogate reproduces the FE stress field with a correlation coefficient r=0.908and an RMSE of 0.058MPa on the 16×16 evaluation grid. The predicted edge stress concentration factor is K_t=3.2, in close agreement with the FE baseline and consistent with the expected amplification near re-entrant corners.

For eccentrically perforated slabs (eccentricity 1.0m), the surrogate locates the shift of the peak principal stress at 0.98m from the geometric center, whereas FE gives 1.02 m; the offset error is 4.2%, remaining within a few percent across held-out asymmetric layouts.

Running time and speedup ratios reported in the literature, In representative studies of surrogate models for structural stress prediction, trained convolutional surrogate models typically complete a forward propagation in just a few milliseconds on a

standard GPU, and tens to hundreds of milliseconds on a CPU. In contrast, a reference finite element (FE) analysis of the same geometry takes several seconds to several minutes, primarily depending on the mesh density (degrees of freedom), element formula, and linear/iterative solver settings. Under identical conditions (matched geometry, load conditions, and mesh resolution), reported speedups typically range from 10^2 to 10^4, with even larger speedups observed on production-grade fine meshes. These figures still depend on hardware and settings (GPU/CPU model, batch size, compiler/BLAS/cuDNN version) and should therefore be understood as orders of magnitude rather than precise comparisons.4.2 Sources of Error and Directions for Improvement

Error diagnostics indicate three dominant contributors when the surrogate is compared with its FE labels. First, label bias from baseline assumptions, notably the idealization of perfect bonding at interfaces and supports, accounts for the largest share of discrepancies, particularly along restraints where local slip or compliance would relax stresses if modeled explicitly. Second, constitutive linearization in the baseline under shrinkage-dominated loading can under-represent tensile softening and tension-stiffening effects, which propagates to the learned mapping in zones approaching cracking. Third, spatial downsampling from the FE field to the 16×16 grid under-resolves steep gradients at hole edges, introducing aliasing in narrow ligaments. An ablation on validation cases attributes roughly one-third of the error to interface idealizations, about one-quarter to constitutive simplifications, and about one-fifth to discretization, with the remainder due to augmentation bias and optimizer variance.

To reduce these errors, two complementary tracks are effective. On the labeling (FE) side, introduce compliant or spring-bond interfaces to emulate near-edge slip and micro-opening (e.g., normal stiffness $K_{11} \approx 4 \times 10^5$ N/m; shear cap $\tau_{max} \approx 0.4 f_c$), and incorporate crack-aware tension-stiffening or elastoplastic modules so that supervisory fields better reflect stress redistribution. On the learning side, augment the loss with edge-aware gradient terms to preserve near-hole peaks, apply multi-resolution supervision to mitigate downsampling artifacts, and adopt physics-guided regularization or PINN-style constraints to embed equilibrium and constitutive relations directly into training [9]. Together, these measures tighten FE–CNN agreement on high-gradient regions without sacrificing the runtime advantage that motivates the surrogate.

CONCLUSIONS

5.1 Core Achievements

This work establishes a convolutional-neural-network surrogate trained on a parametric finite-element (FE) baseline to predict stress fields in perforated concrete slabs. On held-out symmetric layouts the model attains $r = 0.908$ and RMSE $=$ 0.058MPa, while delivering at least a fifty-fold reduction in evaluation time relative to a high-fidelity FE run. When set against commonly used empirical rules, the approach reduces prediction error by roughly forty percent and supports rapid “what-if” exploration and crack-resistance sizing in large plates with complex perforations. Coverage of asymmetric openings is improved through DCGAN augmentation, and an equilibrium-residual penalty enforces $\nabla \cdot \sigma = 0$ consistency, which stabilizes predictions near re-entrant corners and narrow ligaments. All assessments are

performed against the FE reference, keeping methodology and conclusions within a single, physically consistent frame.

5.2 Future Research Directions

Further gains are expected from enriching the supervisory physics in the FE labels by introducing interface compliance and crack-aware tension-stiffening, coupled with multi-resolution supervision to better resolve near-edge gradients. On the learning side, incorporating physics-guided constraints or PINN-style formulations can embed constitutive behavior during training and reduce bias where tensile softening emerges . Extending the present 2D mapping toward 2.5D/3D settings will enable layered slabs and volumetric openings to be addressed with full through-thickness stress components. For deployment, adding histories of shrinkage, temperature and sustained loading, together with uncertainty quantification and calibration protocols, will make the surrogate suitable for preliminary design while traceable to the FE baseline. Active curation of the dataset, querying regions of high epistemic uncertainty and generating targeted FE cases, offers a practical path to iterative improvement without sacrificing computational efficiency.

REFERENCES

[1] Zhang Hua.Cracking mechanism and prevention technology of large concrete slab holes [J]. Journal of Building Structure，2020,41(5): 123-132.

[2] Li W. Finite Element Analysis of Shrinkage Cracking in Mass Concrete[J]. Computers & Structures,2021,250:106321.

[3] Zhang W. Full-Field Shrinkage Strain Monitoring of Large-Scale Concrete Plates[J].Measurement,2023,223:114098.

[4] Chen G.Experimental Study on Eccentric Hole Effect in Concrete Slabs[J]. Journal of Structural Engineering,ASCE,2020,146(7):04020123.

[5] Sun X.Attention-Based CNN for Stress Concentration Prediction[J]. Computers & Structures,2022,270:106698.

[6] Wang Q.Data Augmentation for Asymmetric Holes Using DCGAN[J]. Computers & Geotechnics,2023,152:104897.

[7] Guo Y.Experimental Study on Stress Concentration of Multi-Opening Plates[J]. Engineering Structures,2022,259:114182.

[8] Li Z.Physics-Informed Neural Networks for Plate Stress Analysis[J]. Applied Mathematics and Mechanics,2022,43(12):1859-1872.